

In Fig. 5, we show the sum throughputs for the proposed LE, the RBF, and the optimal VP using SE as the SNR increases. When the number of users is 50 and 10, the sum throughputs of SE and LE exponentially increase in SNR increments. Meanwhile, the sum throughput of the RBF converges to a certain value because of the lack of MUD. Even in small-user networks (i.e., ten users), the sum throughputs of SE and LE have small losses compared with those of relatively large-user networks (i.e., 50 users). This implies that both SE and LE are able to achieve sufficient MUD, even in small-user networks. In comparison with SE at high SNRs, the proposed LE has a slight throughput loss, which can be considered as not severe because LE has a very low complexity and no throughput convergence. This LE scheme is thus more beneficial to implement within practical systems than is the SE scheme.

Consequently, the encoding complexity of the proposed LE is not far from the linear ZF precoder and is merely a square root of the optimal VP via SE while achieving a reasonable throughput performance within MU-MIMO systems.

V. CONCLUSION

We have proposed a new VP based on LE within the MU-MIMO downlink. Through eigenvalue normalization and a good searching step size, the proposed LE scheme can successfully find the optimal perturbation vector while also greatly reducing the encoding complexity. Analytic and simulation results showed that LE can achieve a competent throughput performance with a very low encoding complexity, which is merely a square root of the optimal VP scheme via SE. Therefore, the proposed LE is a promising precoder to be practically implemented within MU-MIMO systems.

REFERENCES

- [1] G. Caire and S. Shamai, "On the achievable throughput of a multi-antenna Gaussian broadcast channel," *IEEE Trans. Inf. Theory*, vol. 43, no. 7, pp. 1691–1706, Jul. 2003.
- [2] H. Weingarten, Y. Steinberg, and S. Shamai, "The capacity region of the Gaussian multiple-input multiple-output broadcast channel," *IEEE Trans. Inf. Theory*, vol. 52, no. 9, pp. 3946–3964, Sep. 2006.
- [3] M. Sharif and B. Hassibi, "On the capacity of MIMO broadcast channels with partial side information," *IEEE Trans. Inf. Theory*, vol. 51, no. 2, pp. 506–522, Feb. 2005.
- [4] T. Yoo, N. Jindal, and A. Goldsmith, "Multi-antenna downlink channels with limited feedback and user selection," *IEEE J. Sel. Areas Commun.*, vol. 25, no. 7, pp. 1478–1491, Sep. 2007.
- [5] B. M. Hochwald, C. B. Peel, and A. L. Swindlehurst, "A vector-perturbation technique for near-capacity multi-antenna multi-user communication—Part II: Perturbation," *IEEE Trans. Commun.*, vol. 53, no. 3, pp. 537–544, Mar. 2005.
- [6] C. Windpassinger, R. F. H. Fischer, and J. B. Huber, "Lattice-reduction-aided broadcast precoding," *IEEE Trans. Commun.*, vol. 52, no. 12, pp. 2057–2060, Dec. 2004.
- [7] E. Ko and D. Hong, "A robust STBC-based transmit diversity scheme for OFDM systems over spatially transmit correlated fading channels," *IEEE Trans. Veh. Technol.*, vol. 56, no. 2, pp. 984–991, Mar. 2007.
- [8] O. Damen, A. Chkeif, and J.-C. Belfiore, "Lattice code decoder for space-time codes," *IEEE Commun. Lett.*, vol. 4, no. 5, pp. 161–163, May 2000.
- [9] B. Hassibi and H. Vikalo, "On the sphere-decoding algorithm I. Expected complexity," *IEEE Trans. Signal Process.*, vol. 53, no. 8, pp. 2806–2818, Aug. 2005.
- [10] J. Fu, T. Taniguchi, and Y. Karasawa, "The largest eigenvalue characteristics for MIMO channels with spatial correlation," *Electron. Commun. Jpn.*, vol. 87, pt. 1, no. 12, pp. 18–27, Dec. 2004.
- [11] J. Salo, D. Seethaler, and A. Skupch, "On the asymptotic geometric mean of MIMO channel eigenvalues," in *Proc. IEEE Int. Symp. Inf. Theory*, Jul. 2006, pp. 2109–2113.

Generalized MBER-Based Vector Precoding Design for Multiuser Transmission

Wang Yao, Sheng Chen, *Fellow, IEEE*, and Lajos Hanzo, *Fellow, IEEE*

Abstract—We propose a generalized vector precoding (VP) design based on the minimum bit error rate (MBER) criterion for multiuser transmission in the downlink of a multiuser system, where the base station (BS) equipped with multiple transmitting antennas communicates with single-receiving-antenna mobile station (MS) receivers each having a modulo device. Given the knowledge of the channel state information and the current information symbol vector to be transmitted, our scheme directly generates the effective symbol vector based on the MBER criterion using the particle swarm optimization (PSO) algorithm. The proposed PSO-aided generalized MBER VP scheme is shown to outperform the powerful minimum mean-square-error (MMSE) VP and improved MMSE-VP benchmarks, particularly for rank-deficient systems, where the number of BS transmitting antennas is lower than the number of MSs supported.

Index Terms—Minimum bit error rate (MBER), minimum mean square error (MMSE), multiuser transmission (MUT), particle swarm optimization (PSO), vector precoding (VP).

I. INTRODUCTION

Multiuser detection is effective for mitigating the multiuser interference in the uplink (UL), but its employment is infeasible in the downlink (DL) of a space-division multiple-access (SDMA) system supporting noncooperative mobile stations (MSs). To employ a low-complexity high-power-efficiency single-user MS receiver, the transmitted multiuser DL signals may be preprocessed at the base station (BS), leading to the concept of multiuser transmission (MUT) [1], [2], provided that the MS's DL channels are known at the BS. More explicitly, MUT requires the knowledge of each user's unique channel impulse response (CIR) for differentiating the different users' transmissions. In time-division duplex systems, the UL CIRs measured at the BS may be used for the subsequent DL preprocessing by exploiting the channel's reciprocity, provided that both the noise and the cochannel interference are similar at the BS and MSs. Feeding back the CIR from the MS's receivers to the BS transmitter is, however, necessary for frequency-division duplex systems, where the UL and DL channels are different, since they are at different frequency bands. MUT schemes can be divided into linear and nonlinear MUT families, respectively.

The well-known linear MUT methods include the zero-forcing (ZF) and minimum mean-square-error (MMSE) MUT schemes [1], [2], which have an appealing simplicity but exhibit a limited bit error rate (BER) performance. Various symbol-specific linear minimum BER (MBER) MUT schemes were proposed for enhancing the system's achievable BER performance [3]–[6], where the precoding weights are specifically designed for the given transmit symbol vector, and therefore, the coefficients of the precoder have to be calculated for every transmit symbol vector. A linear MBER-MUT minimizing the

Manuscript received May 12, 2010; revised October 1, 2010; accepted November 23, 2010. Date of publication December 10, 2010; date of current version February 18, 2011. The review of this paper was coordinated by Dr. C.-C. Chong.

The authors are with the School of Electronics and Computer Science, University of Southampton, SO17 1BJ Southampton, U.K. (e-mail: wy07r@ecs.soton.ac.uk; sqc@ecs.soton.ac.uk; lh@ecs.soton.ac.uk).

Color versions of one or more of the figures in this paper are available online at <http://ieeexplore.ieee.org>.

Digital Object Identifier 10.1109/TVT.2010.2098428

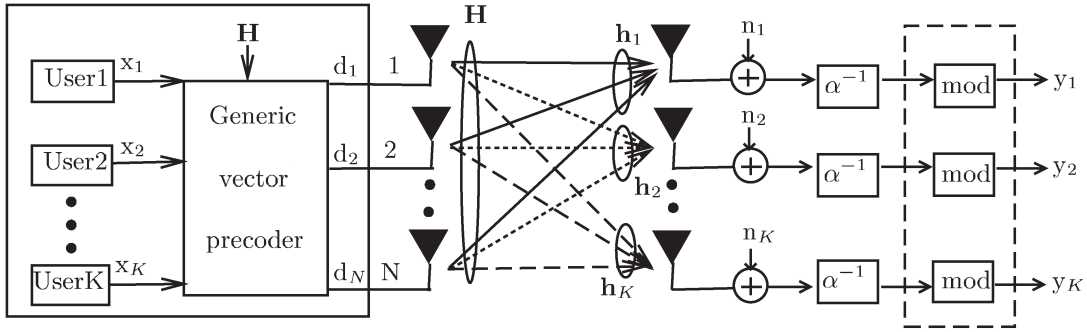


Fig. 1. Schematic diagram of the SDMA system's DL using preprocessing at the BS. The MUT-aided system employs N transmitting antennas at the BS to communicate with K noncooperative single-receiving-antenna MSs each with a modulo device.

average BER was proposed for both binary phase-shift-keying modulation [7] and 4-quadrature amplitude modulation (4-QAM) [8], where the coefficients of the precoder only had to be recalculated when the channel coefficients changed substantially, which is determined by the Doppler frequency. The solutions of [8] and [9] proposed attractive low-complexity particle swarm optimization (PSO)-aided MBER MUT designs.

Nonlinear MUT techniques are capable of approaching the rate region of dirty paper coding [10]. Specifically, the vector precoding (VP) algorithm of [11]–[15], where each receiver employs a modulo device, is capable of outperforming any linear preprocessing technique in terms of the system's achievable BER. The VP of [12] was based on the ZF criterion, whereas the more powerful MMSE-VP solution was derived later in [13]. The authors of [14] proposed a VP precoder design, where the data vector to be transmitted is perturbed by an arbitrary vector to minimize the total MSE, whereas the VP technique of [15] determines a continuous-valued perturbation vector that minimizes the MSE of the received signal. Although numerous different MMSE-VP techniques have been proposed [13]–[15], the solution advocated in [13] was deemed to be the predominant MMSE-VP scheme [16]–[18]. The authors of [19] analyzed an MMSE-VP, where the receiver can replace the modulo device with the statistics of perturbation. More recently, an improved MMSE-VP (ImMMSE-VP) scheme was developed in [20]. In this ImMMSE-VP, the precoding matrix is designed based on the MMSE criterion, just as the MMSE-VP of [13] does, but it obtains the perturbation vector based on the MBER criterion, whereas the MMSE-VP scheme of [13] derives the perturbation vector based on the MMSE criterion.

Against this background, in this paper, we propose an advanced VP design directly and fully based on the MBER criterion. To the best of our knowledge, no such VP algorithm was proposed in the literature before. Our novel contributions are as follows.

- 1) Given the knowledge of the information symbol vector and the channel matrix, conventional VP algorithms, such as [13] and [20], determine the precoding matrix and the perturbation vector separately, which are then used to generate the effective symbol vector to be transmitted. Our scheme, however, directly generates the effective symbol vector to be transmitted based fully on the MBER criterion. Therefore, our proposed scheme is referred to as the generalized MBER-based VP (GMBER-VP).
- 2) Since the resultant design constitutes a nonconvex continuous-valued optimization problem, we adopt the computationally efficient PSO algorithm [9], [21]–[23] to create the generalized MBER VP design. Our complexity study demonstrates that the complexity imposed by the GMBER-VP design is only slightly higher than that of the ImMMSE-VP scheme and is no higher than twice that of the MMSE-VP solution.

- 3) We demonstrate that the proposed GMBER-VP algorithm outperforms the powerful MMSE-VP proposed in [13] and the ImMMSE-VP in [20], particularly for rank-deficient systems, where the number of BS transmitting antennas is lower than the number of MSs supported.

For ease of reference, the abbreviations used to represent all the three algorithms compared in this paper are briefly explained as follows.

- 1) MMSE-VP [13]: This is a conventional two-step VP design. The precoding matrix and the perturbation vector are first chosen separately to minimize the system's mean square error (MSE), which are then used to generate the effective symbol vector to be transmitted.
- 2) ImMMSE-VP [20]: This is also a two-step design. The scheme generates the MMSE-based precoding matrix, as the MMSE-VP scheme does, but it determines the discrete-valued perturbation vector by minimizing the BER. The resultant precoding matrix and perturbation vector are then used to generate the effective symbol vector to be transmitted.
- 3) GMBER-VP: This is the proposed generalized MBER-based VP design in which the effective symbol vector to be transmitted is directly generated to minimize the system's BER.

The following notational conventions are adopted throughout this paper. Boldface capitals and lowercase letters stand for matrices and vectors, respectively. Furthermore, $()^T$ represents the transpose operator, whereas $\|\cdot\|^2$ and $|\cdot|$ denote the norm and the magnitude operators, respectively. $E[\cdot]$ denotes the expectation operator, whereas $\Re[\cdot]$ and $\Im[\cdot]$ represent the real and imaginary parts, respectively. Finally, $j = \sqrt{-1}$.

II. SYSTEM MODEL

The DL of an SDMA system is depicted Fig. 1, where the BS equipped with N transmitting antennas communicates over frequency-flat fading channels with K noncooperative MSs, each employing a single receiving antenna and a modulo device. Note that frequency-selective channels can be rendered nondispersive using, for example, the orthogonal frequency-division-multiplexing technique [24]. The DL channel matrix \mathbf{H} of the system is given by

$$\mathbf{H} = [\mathbf{h}_1 \quad \mathbf{h}_2 \quad \cdots \quad \mathbf{h}_K] \quad (1)$$

where $\mathbf{h}_k = [h_{1,k} \quad h_{2,k} \quad \cdots \quad h_{N,k}]^T$, $1 \leq k \leq K$ is the k th user's spatial signature. The nondispersive CIR taps $h_{i,k}$ for $1 \leq k \leq K$ and $1 \leq i \leq N$ are independent of each other and obey the complex-valued Gaussian distribution with $E[|h_{i,k}|^2] = 1$. The K -element information symbol vector to be transmitted to the K MSs is given

by $\mathbf{x} = [x_1 \ x_2 \ \dots \ x_K]^T$, where x_k is the information symbol destined for the k th MS. Given \mathbf{x} and \mathbf{H} , the generic VP generates the N -element continuous-valued effective symbol vector $\mathbf{d} = [d_1 \ d_2 \ \dots \ d_N]^T$ based on some criterion. In a conventional VP, such as the MMSE-VP [13] or the ImMMSE-VP [20], the $(N \times K)$ precoding matrix \mathbf{P} and the K -element discrete- or continuous-valued perturbation vector $\boldsymbol{\omega}$ are separately determined based on \mathbf{H} and \mathbf{x} . The effective symbol vector \mathbf{d} is then expressed as

$$\mathbf{d} = \mathbf{P}(\mathbf{x} + \boldsymbol{\omega}). \quad (2)$$

Our proposed scheme, however, does not determine \mathbf{P} and $\boldsymbol{\omega}$. Rather, it directly determines \mathbf{d} , and therefore, it is referred to as the generalized VP precoder.

The DL channel noise vector is defined by $\mathbf{n} = [n_1 \ n_2 \ \dots \ n_K]^T$, where n_k , $1 \leq k \leq K$, is a complex-valued Gaussian white noise process with $E[|n_k|^2] = 2\sigma_n^2 = N_o$. Given a fixed total transmitting power E_T at the BS, an appropriate scaling factor is used to fulfill this transmitting power constraint, which is defined as $\alpha = \sqrt{E_T/\|\mathbf{d}\|^2}$. At the receiver, the reciprocal of the scaling factor, namely, α^{-1} , is used to scale the received signal to maintain a unity-gain transmission. The energy per bit per antenna is given by $E_b = E_T/N \log_2 M$ for the M -ary modulation considered. The SNR is defined as $\text{SNR} = E_b/N_o$. The received signal vector $\hat{\mathbf{y}} = [\hat{y}_1 \ \hat{y}_2 \ \dots \ \hat{y}_K]^T$ before the modulo operation is given by

$$\hat{\mathbf{y}} = \mathbf{H}^T \mathbf{d} + \alpha^{-1} \mathbf{n}. \quad (3)$$

The modulo operation invoked for \hat{y}_k is described by [12]

$$\text{mod}_\tau(\hat{y}_k) = \hat{y}_k - \left\lfloor \frac{\Re[\hat{y}_k] + \tau/2}{\tau} \right\rfloor \tau - j \left\lfloor \frac{\Im[\hat{y}_k] + \tau/2}{\tau} \right\rfloor \tau \quad (4)$$

where $1 \leq k \leq K$, $\lfloor \bullet \rfloor$ denotes the integer floor operator, and τ is a positive number determined by the modulation constellation employed. The received signal vector $\mathbf{y} = [y_1 \ y_2 \ \dots \ y_K]^T$ after the modulo operation is given by

$$\mathbf{y} = \text{mod}_\tau(\hat{\mathbf{y}}) \quad (5)$$

and y_k , $1 \leq k \leq K$ constitutes sufficient statistics for the k th MS to detect the transmitted information data symbol x_k . The authors of [12] suggested to choose τ according to

$$\tau = 2(|c|_{\max} + \Delta/2) \quad (6)$$

where $|c|_{\max}$ is the largest distance of the modulated symbols to the real or imaginary axis, and Δ is the spacing between the constellation points. Specifically, consider a 4-QAM scheme, where the four symbols all have the amplitude of $\sqrt{2}/2$. The values of $|c|_{\max}$ and Δ are given by $|c|_{\max} = 1/2$ and $\Delta = 1$, respectively. Thus, we have $\tau = 2$ according to (6). The modulo operator (4) maps the received signal $\Re[\hat{y}_k]$ and $\Im[\hat{y}_k]$ into the interval $[-\tau/2, \tau/2)$. For example, if $\Re[\hat{y}_k] = 1.75\tau$, it is then mapped to $\Re[y_k] = -0.25\tau$ by the modulo operation.

III. MINIMUM BIT ERROR RATE GENERALIZED VECTOR PRECODER DESIGN

For notational simplicity, we consider a 4-QAM scheme having $M = 4$. Extensions to a high-order QAM scheme can be achieved

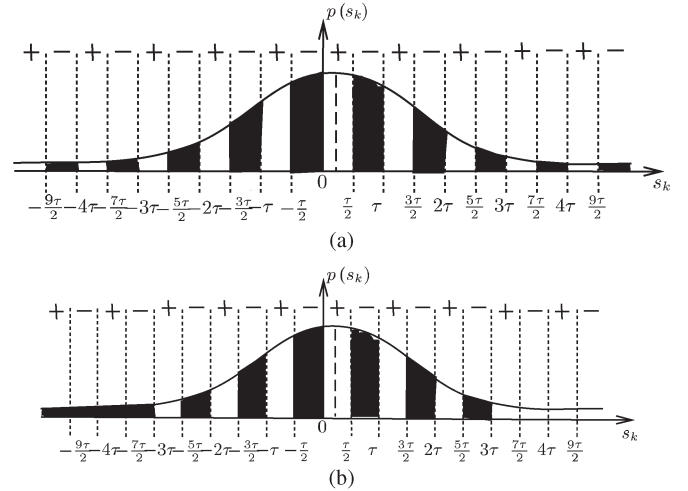


Fig. 2. PDF of the decision variable s_k . (a) Shaded areas represent the exact BER. (b) Shaded areas represent the approximate BER.

by considering the minimum symbol error rate criterion, as in the multiuser detector of [25]. The error probability or BER encountered at the output of the receiver after the modulo operation for the in-phase component of user k is defined by

$$P_{e_I,k}(\mathbf{d}) = \text{Prob} \{ \text{sgn}(\Re[x_k]) \Re[y_k] < 0 \}. \quad (7)$$

Define the signed decision variable $s_k = \text{sgn}(\Re[x_k]) \Re[y_k]$, which has the probability density function (pdf) given by

$$p(s_k) = \frac{1}{\sqrt{2\pi}\alpha^{-1}\sigma_n} \exp\left(-\frac{(s_k - c_R^{(k)})^2}{2\sigma_n^2\alpha^{-2}}\right) \quad (8)$$

with the mean $c_R^{(k)} = \text{sgn}(\Re[x_k]) \Re[\mathbf{h}_k^T \mathbf{d}]$. Note that the decision areas are periodically extended in the s_k -axis, as illustrated in Fig. 2, where the intervals marked by $-$ are the error areas, i.e., $\text{sgn}(\Re[x_k]) \Re[y_k] < 0$, whereas the intervals marked by $+$ are the error-free areas, i.e., $\text{sgn}(\Re[x_k]) \Re[y_k] > 0$. A decision error occurs when s_k falls into the intervals $[(2m+1/2)\tau, (m+1)\tau)$ for $-\infty < m < \infty$. Therefore, the BER of the in-phase component associated with user k is

$$\begin{aligned} P_{e_I,k}(\mathbf{d}) &= \sum_{m=-\infty}^{\infty} \int_{\frac{2m+1}{2}\tau}^{(m+1)\tau} p(s_k) ds_k \\ &\approx \int_{-\infty}^{-3\tau} p(s_k) ds_k + \int_{-\frac{5\tau}{2}}^{-2\tau} p(s_k) ds_k + \int_{-\frac{3\tau}{2}}^{-\tau} p(s_k) ds_k \\ &\quad + \int_{-\frac{\tau}{2}}^0 p(s_k) ds_k + \int_{\frac{\tau}{2}}^{\tau} p(s_k) ds_k \\ &\quad + \int_{\frac{3\tau}{2}}^{2\tau} p(s_k) ds_k + \int_{\frac{5\tau}{2}}^{3\tau} p(s_k) ds_k \end{aligned} \quad (9)$$

where the approximation occurs as we lump the integrations over all the error intervals in $(-\infty, -3\tau)$ and $(3\tau, +\infty)$ together as the

single integration over the interval $(-\infty, -3\tau)$. This approximation is accurate owing to the near symmetry of the pdf [see (8)] in the two regions $(3\tau, +\infty)$ and $(-\infty, -3\tau)$. Furthermore, the last six integrations at the right-hand side of the approximation are much larger than the first term. The true BER $P_{e_I,k}(\mathbf{d})$ and its approximation are illustrated in Fig. 2(a) and (b), respectively. $P_{e_I,k}(\mathbf{d})$ can further be expressed as

$$\begin{aligned}
P_{e_I,k}(\mathbf{d}) \approx & Q\left(\frac{c_R^{(k)} + 3\tau}{\alpha^{-1}\sigma_n}\right) + Q\left(\frac{-\frac{5\tau}{2} - c_R^{(k)}}{\alpha^{-1}\sigma_n}\right) \\
& - Q\left(\frac{-2\tau - c_R^{(k)}}{\alpha^{-1}\sigma_n}\right) + Q\left(\frac{-\frac{3\tau}{2} - c_R^{(k)}}{\alpha^{-1}\sigma_n}\right) \\
& - Q\left(\frac{-\tau - c_R^{(k)}}{\alpha^{-1}\sigma_n}\right) + Q\left(\frac{-\frac{\tau}{2} - c_R^{(k)}}{\alpha^{-1}\sigma_n}\right) \\
& - Q\left(\frac{-c_R^{(k)}}{\alpha^{-1}\sigma_n}\right) + Q\left(\frac{\frac{\tau}{2} - c_R^{(k)}}{\alpha^{-1}\sigma_n}\right) \\
& - Q\left(\frac{\tau - c_R^{(k)}}{\alpha^{-1}\sigma_n}\right) + Q\left(\frac{\frac{3\tau}{2} - c_R^{(k)}}{\alpha^{-1}\sigma_n}\right) \\
& - Q\left(\frac{2\tau - c_R^{(k)}}{\alpha^{-1}\sigma_n}\right) + Q\left(\frac{\frac{5\tau}{2} - c_R^{(k)}}{\alpha^{-1}\sigma_n}\right) \\
& - Q\left(\frac{3\tau - c_R^{(k)}}{\alpha^{-1}\sigma_n}\right)
\end{aligned} \quad (10)$$

where $Q(\cdot)$ is the standard Gaussian error function. Hence, the average BER of the in-phase component of \mathbf{y} at the receivers is given by

$$P_{e_I,\mathbf{x}}(\mathbf{d}) = \frac{1}{K} \sum_{k=1}^K P_{e_I,k}(\mathbf{d}). \quad (11)$$

Similarly, let $c_I^{(k)} = \text{sgn}(\Im[x_k])\Im[\mathbf{h}_k^T \mathbf{d}]$. Then, the BER of the quadrature-phase component for the k th user, which is denoted as $P_{e_Q,k}(\mathbf{d})$, takes the same form of $P_{e_I,k}(\mathbf{d})$ and can be derived by replacing $c_R^{(k)}$ with $c_I^{(k)}$ in (10). Then, the average BER of the quadrature-phase component of \mathbf{y} at the receivers of the K MSs is given by

$$P_{e_Q,\mathbf{x}}(\mathbf{d}) = \frac{1}{K} \sum_{k=1}^K P_{e_Q,k}(\mathbf{d}). \quad (12)$$

The resultant average BER for 4-QAM signaling becomes

$$P_{e,\mathbf{x}}(\mathbf{d}) = (P_{e_I,\mathbf{x}}(\mathbf{d}) + P_{e_Q,\mathbf{x}}(\mathbf{d}))/2. \quad (13)$$

Hence, the optimal continuous-valued effective symbol vector \mathbf{d}_{opt} is found by solving the following optimization problem:

$$\mathbf{d}_{\text{opt}} = \arg \min_{\mathbf{d}} P_{e,\mathbf{x}}(\mathbf{d}). \quad (14)$$

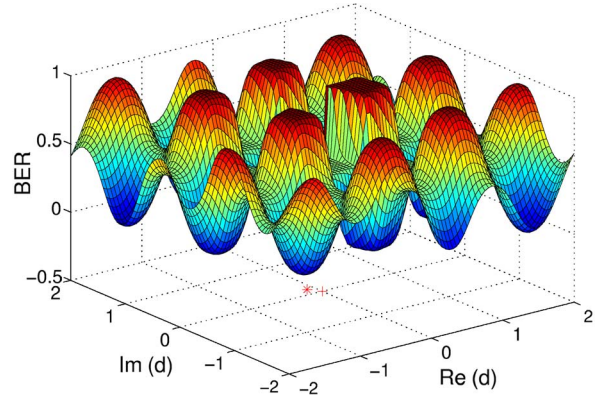


Fig. 3. BER surface as a function of the effective symbol vector \mathbf{d} for the simplest 4-QAM system with $N = 1$ and $K = 1$ given SNR = 16 dB. The mark * indicates the GMBER-VP solution, whereas the mark + is the MMSE-VP solution.

Note that the average BER [see (13)], which is a function of the effective symbol vector to be transmitted, is very different from the average BER¹ used in [20].

IV. PARTICLE SWARM OPTIMIZATION AIDED MINIMUM BIT ERROR RATE GENERALIZED VP DESIGN

The optimization problem [see (14)] is a challenging nonconvex optimization problem, where many local minimas exist, particularly at high SNR values. As an illustration, Fig. 3 depicts the BER surface $P_{e,\mathbf{x}}(\mathbf{d})$ for the simplest case of $N = 1$ and $K = 1$ at SNR = 16 dB. We propose to solve the GMBER-VP design problem [see (14)] using the PSO algorithm [21]. PSO constitutes a population-based stochastic optimization technique inspired by the social behavior of bird flocks or fish schools. The algorithm commences with the random initialization of a swarm of individuals, which are referred to as particles, within the problem's search space. Each particle then gradually adjusts its trajectory with the aid of cognitive information (its own best location) and social information (the best position of the entire swarm) at each iteration. PSO is simple to implement, has the ability to rapidly converge, and is capable of steering clear of local minima. Wide-ranging engineering applications based on PSO [8], [22], [23], [26]–[28] have demonstrated the ability of PSO to attain global or near-global optimal solutions at affordable computational costs.

In our algorithm, a swarm of particles $\{\mathbf{d}_i^{(l)}\}_{i=1}^S$ that represent potential solutions is evolved in the search space \mathcal{D}^N , where S is the swarm size, l denotes the iteration index, and

$$\mathcal{D} = [-P_{\max}, P_{\max}] + j[-P_{\max}, P_{\max}] \quad (15)$$

specifies the search range for each element of \mathbf{d} .

- a) Initialization. Set $l = 0$, choose $\mathbf{d}_1^{(l)}$ to be the solution of the ImMMSE-VP scheme² given in [20], and generate the rest of the particles $\{\mathbf{d}_i^{(l)}\}_{i=2}^S$ randomly in \mathcal{D}^N .

¹In fact, in the ImMMSE-VP design [20], the average BER is defined as the function of the discrete-valued perturbation vector $\boldsymbol{\omega}$, given the information symbol vector \mathbf{x} and the MMSE-based precoding matrix \mathbf{P} . After finding the MBER solution for $\boldsymbol{\omega}$, the effective symbol vector to be transmitted is then obtained according to (2).

²The reason for choosing this initialization is to improve the probability of finding the global optimal solution and to enhance the convergence speed. Other initialization, such as using the MMSE-VP solution given in [13], may also be adopted.

- b) Evaluation. Each particle $\mathbf{d}_i^{(l)}$ has an associated cost $P_{e,x}(\mathbf{d}_i^{(l)})$. Each particle $\mathbf{d}_i^{(l)}$ remembers its best position visited, which is denoted as $\mathbf{pb}_i^{(l)}$, which provides the cognitive information. Every particle also knows the best position visited among the entire swarm, denoted as $\mathbf{gb}^{(l)}$, which provides the social information. The cognitive information $\{\mathbf{pb}_i^{(l)}\}_{i=1}^S$ and the social information $\mathbf{gb}^{(l)}$ are updated at each iteration, given the new cost information $\{P_{e,x}(\mathbf{d}_i^{(l)})\}_{i=1}^S$.
- c) Update. Each particle $\mathbf{d}_i^{(l)}$ has a velocity $\mathbf{v}_i^{(l)}$ to direct its “flight” or search. The velocity and position of the i th particle are updated in each iteration according to

$$\begin{aligned} \mathbf{v}_i^{(l+1)} = & w_1 * \mathbf{v}_i^{(l)} + c_1 * \varphi_1 * (\mathbf{pb}_i^{(l)} - \mathbf{d}_i^{(l)}) \\ & + c_2 * \varphi_2 * (\mathbf{gb}^{(l)} - \mathbf{d}_i^{(l)}) \end{aligned} \quad (16)$$

$$\mathbf{d}_i^{(l+1)} = \mathbf{d}_i^{(l)} + \mathbf{v}_i^{(l+1)} \quad (17)$$

where w_1 is the inertia weight and c_1 and c_2 are the two acceleration coefficients, whereas $\varphi_1 = \text{rand}()$ and $\varphi_2 = \text{rand}()$ denote the two random variables uniformly distributed in $(0, 1)$. To avoid excessive roaming of particles beyond the search space, a velocity space V^N with

$$V = [-V_{\max}, V_{\max}] + j[-V_{\max}, V_{\max}] \quad (18)$$

is imposed so that each element of $\mathbf{v}_i^{(l+1)}$ is forced back into the velocity range V defined in (18). Similarly, if a particle $\mathbf{d}_i^{(l+1)}$ moves outside the search space, then it is randomly moved back into a position inside the search space.

- d) Termination. If the maximum number of iterations I_{\max} is reached, then terminate the algorithm with the solution $\mathbf{d}_{\text{opt}} = \mathbf{gb}^{(I_{\max})}$; otherwise, set $l = l + 1$, and go to Step b).

The search range [see (15)] is specified by the optimization problem. For 4-QAM signaling, our extensive empirical results show that the magnitudes of $\Re[d_k]$ and $\Im[d_k]$ obtained by the MMSE-VP solution are typically smaller than 1.0, although occasionally, they may be slightly larger than 1.0. This observation is also true for the proposed GMBER-VP design. Therefore, we set $P_{\max} = 1.2$. The velocity limit V_{\max} is typically related to P_{\max} , and we empirically set $V_{\max} = 0.2$. The inertia weight is chosen as $w_1 = \text{rand}()$, which was seen to perform better in our application than the two alternative choices of opting for $w_1 = 0$ and setting w_1 to a small positive constant. The time-varying acceleration coefficients [23], in which c_1 is reduced from 2.5 to 0.5 and c_2 varies from 0.5 to 2.5 during the iterative procedure according to

$$c_1 = (0.5 - 2.5) * l / I_{\max} + 2.5, c_2 = (2.5 - 0.5) * l / I_{\max} + 0.5 \quad (19)$$

were also shown to perform well in our application. Appropriate values for S and I_{\max} are chosen to ensure that the algorithm converges to a global solution with a minimum complexity.

In Step a), one of the particles is initialized to be the ImMMSE-VP solution of [20]. The complexity of obtaining the ImMMSE-VP solution is given by

$$C_{\text{ImMMSE-VP}} = (73K + 18KN + 6N + 4)D \quad (20)$$

where N is the number of the BS transmitting antennas, K is the number of MSs supported, and D is the extended constellation points

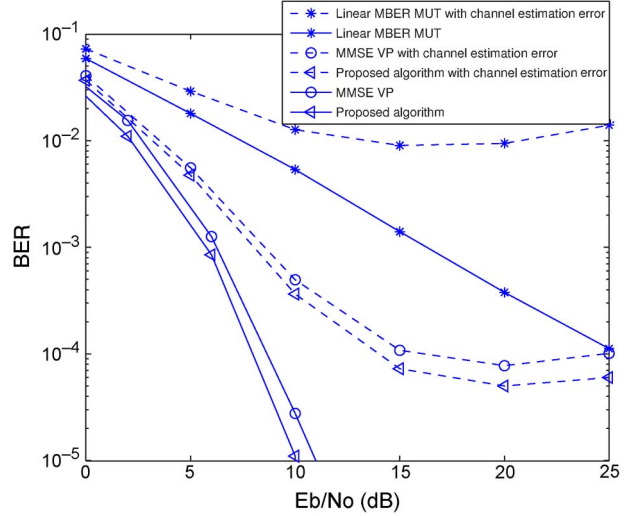


Fig. 4. Performance comparison of the MMSE-VP [13], the ImMMSE-VP [20], and our proposed PSO-aided GMBER-VP for communicating over flat Rayleigh fading channels using $N = 4$ transmitting antennas to support $K = 4$ 4-QAM users.

visited in determining the discrete-valued perturbation vector [13], [20]. The complexity of the PSO-aided GMBER-VP design may be shown to be

$$\begin{aligned} C_{\text{GMBER-VP}} = & (7N + (73 + 7N)K \\ & + (23N + (73 + 7N)K + 6) I_{\max}) S \\ & + (73K + 18KN + 6N + 4)D \\ & + 2K + 7KN + 5S \end{aligned} \quad (21)$$

where S is the swarm size, and I_{\max} is the number of iterations that the algorithm requires to converge. As a comparison, the complexity of the MMSE-VP design [13] is given by

$$\begin{aligned} C_{\text{MMSE-VP}} = & \left(\frac{7}{3}K^3 + 13K^2 + 13K - 1 \right) D \\ & + \mathcal{O}(9K^2N^2 - 2K^2) \end{aligned} \quad (22)$$

where $\mathcal{O}()$ denotes the order of complexity. In the following complexity comparison, we simply set $\mathcal{O}(9K^2N^2 - 2K^2) = 9K^2N^2 - 2K^2$.

V. SIMULATION RESULTS

We considered the DL of a multiuser system employing N transmitting antennas at the BS to support K 4-QAM MSs. All the results were averaged over 100 channel realizations. The appropriate swarm size was empirically found to be $S = 20$, and the maximum number of iterations ranged from $I_{\max} = 20$ to 45, depending on the specific system and SNR value.

- a) Full-rank system. We considered the case of $N = 4$ and $K = 4$. First, perfect knowledge of the DL CIR matrix was assumed at the BS. It can be seen from Fig. 4 that the proposed PSO-aided GMBER-VP scheme achieved 1-dB SNR gain at the target BER of 10^{-5} over the MMSE-VP and the ImMMSE-VP. For this full-rank system, the ImMMSE-VP and the MMSE-VP achieved identical BER performance, which was also

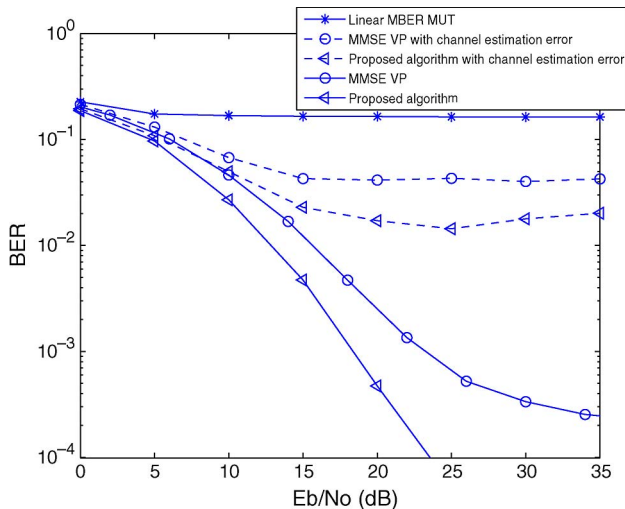


Fig. 5. Performance comparison of the MMSE-VP [13], the ImMMSE-VP [20], and our proposed PSO-aided GMBER-VP for communicating over flat Rayleigh fading channels using $N = 2$ transmitting antennas to support $K = 4$ 4-QAM users.

observed in [20]. The robustness of the three algorithms against the channel estimation error was investigated next. A complex-valued Gaussian white noise with a variance of 0.01 was added to each channel tap $h_{i,k}$ to represent the channel estimation error, and the BERs of these three VP designs under this channel estimation error were also depicted in Fig. 4, where it can be seen that the GMBER-VP design was no more sensitive to channel estimation errors than the MMSE-VP and the ImMMSE-VP designs.

- b) Rank-deficient system. The system was then tuned to use $N = 2$ transmitting antennas to support $K = 4$ 4-QAM users, which was a challenging rank-deficient scenario. The BERs of the three algorithms assuming perfect knowledge of the channel matrix, as well as the performance of the three VP schemes under the same channel estimation error as specified in the previous example, are shown in Fig. 5. The MMSE-VP scheme encountered an error floor since it was unable to differentiate the users' information in this demanding scenario. The ImMMSE-VP design showed a much better performance but still suffered from a visible error floor, as seen in Fig. 5. By contrast, GMBER-VP outperformed the other two designs, and as a further benefit, it did not exhibit a visible error floor, which showed its ability to successfully operate in the rank-deficient scenario. Furthermore, the GMBER-VP algorithm was seen to be no more sensitive to channel estimation errors than the other two designs.

Next, we showed that our choice of swarm size $S = 20$ for the PSO algorithm was a reasonable good choice in terms of complexity. Fig. 6 shows that $S = 10$ was insufficient for the PSO algorithm, whereas the PSO algorithms of $S = 20, 30,$ and 40 all converged to the optimal solution with $I_{\max} = 40, 32,$ and $25,$ respectively. Thus, the required complexity was 4 065 148 (Flops), 4 149 838 (Flops), and 4 174 288 (Flops), corresponding to $S = 20, 30,$ and $40,$ respectively. This confirms that the choice of $S = 20$ was optimal in this case.

The computational complexity of the three VP designs was then compared. Given $\text{SNR} = 25$ dB, the PSO-aided GMBER-VP solution associated with $S = 20$ and $I_{\max} = 40$ imposed a complexity of 4 065 148 (Flops) with a recorded run time of 8878.9 s. As a comparison, the MMSE-VP solution imposed a complexity of 2 508 538 (Flops) with an associated run time of 4787.3 s, whereas the complex-

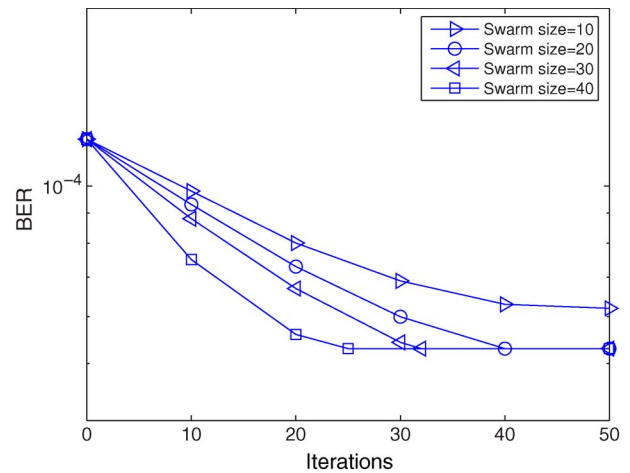


Fig. 6. Convergence of the PSO-aided GMBER-VP algorithm with different swarm sizes S for the rank-deficient system of $N = 2$ and $K = 4$ given the SNR value of 25 dB.

ity of the ImMMSE-VP scheme was 3 654 688 (Flops) with a recorded run time of 7276.2 s. For $\text{SNR} = 30$ dB, the complexity of finding the MMSE-VP solution was 2 609 400 (Flops) with a recorded run time of 4981.9 s and the ImMMSE-VP solution imposed a complexity of 4 010 368 (Flops) with an associated run time of 7522.8 s, whereas the PSO-aided GMBER-VP algorithm associated with $S = 20$ converged to the GMBER-VP solution after $I_{\max} = 45$, which recorded a run time of 9565.8 (s) with an associated complexity of 4 471 028 (Flops). It then becomes clear that for this example, the complexity of the PSO-aided GMBER-VP design was no more than twice of the conventional MMSE-VP design, and it only imposed a slightly higher complexity than that of the ImMMSE-VP benchmark.

VI. CONCLUSION

We have proposed a PSO-aided generalized MBER VP scheme for the DL of a multiuser system, where the BS equipped with multiple transmitting antennas communicates with single-antenna MS receivers, each equipped with a modulo device. Our PSO-aided GMBER-VP design directly generates the effective symbol vector based on the MBER criterion with the knowledge of the DL CIR matrix and the current information symbol vector to be transmitted. Simulation results have shown that our PSO-aided GMBER-VP scheme outperforms the powerful MMSE-VP and ImMMSE-VP schemes, particularly in the challenging rank-deficient scenario, at the modestly increased cost of no more than twice the complexity of the MMSE-VP benchmark.

REFERENCES

- [1] B. R. Vojčić and W. M. Jang, "Transmitter precoding in synchronous multiuser communications," *IEEE Trans. Commun.*, vol. 46, no. 10, pp. 1346–1355, Oct. 1998.
- [2] D. Yang, L.-L. Yang, and L. Hanzo, "Performance of SDMA systems using transmitter preprocessing based on noisy feedback of vector-quantized channel impulse responses," in *Proc. VTC—Spring*, Dublin, Ireland, Apr. 22–25, 2007, pp. 2119–2123.
- [3] R. Irmer, W. Rave, and G. Fettweis, "Minimum BER transmission for TDD-CDMA in frequency-selective channels," in *Proc. PIMRC*, Beijing, China, Sep. 7–10, 2003, vol. 2, pp. 1260–1264.
- [4] R. Irmer, R. Habendorf, W. Rave, and G. Fettweis, "Nonlinear chip-level multiuser transmission for TDD-CDMA with frequency-selective MIMO channels," in *Proc. 5th Int. ITG Conf. Source Channel Coding*, Erlangen, Germany, Jan. 14–16, 2004, pp. 363–370.

- [5] R. Habendorf and G. Fettweis, "Nonlinear optimization for the multiuser downlink," in *Proc. 13th Eur. Wireless Conf.*, Paris, France, Apr. 1–4, 2007.
- [6] F. Richter, A. Fischer, R. Habendorf, and G. Fettweis, "Transmitter-based minimization of error rates in the downlink of wireless systems," in *Proc. GLOBECOM*, New Orleans, LA, Nov. 30–Dec. 4, 2008, pp. 1–5.
- [7] A. Hjørungnes and P. S. R. Diniz, "Minimum BER prefilter transform for communications systems with binary signaling and known FIR MIMO channel," *IEEE Signal Process. Lett.*, vol. 12, no. 3, pp. 234–237, Mar. 2005.
- [8] W. Yao, S. Chen, S. Tan, and L. Hanzo, "Particle swarm optimisation aided minimum bit error rate multiuser transmission," in *Proc. ICC*, Dresden, Germany, Jun. 14–18, 2009, pp. 1–5.
- [9] W. Yao, S. Chen, S. Tan, and L. Hanzo, "Minimum bit error rate multiuser transmission designs using particle swarm optimisation," *IEEE Trans. Wireless Commun.*, vol. 8, no. 10, pp. 5012–5017, Oct. 2009.
- [10] M. Costa, "Writing on dirty paper," *IEEE Trans. Inf. Theory*, vol. IT-29, no. 3, pp. 439–441, May 1983.
- [11] C. B. Peel, B. M. Hochwald, and A. L. Swindlehurst, "A vector-perturbation technique for near-capacity multiantenna multiuser communication—Part I: Channel inversion and regularization," *IEEE Trans. Commun.*, vol. 53, no. 1, pp. 195–202, Jan. 2005.
- [12] B. M. Hochwald, C. B. Peel, and A. L. Swindlehurst, "A vector-perturbation technique for near-capacity multiantenna multiuser communication—Part II: Perturbation," *IEEE Trans. Commun.*, vol. 53, no. 3, pp. 537–544, Mar. 2005.
- [13] D. A. Schmidt, M. Joham, and W. Utschick, "Minimum mean square error vector precoding," in *Proc. PIMRC*, Berlin, Germany, Sep. 11–14, 2005, vol. 1, pp. 107–111.
- [14] E. Y. Kim and J. Chun, "Optimum vector perturbation minimizing total MSE in multiuser MIMO downlink," in *Proc. ICC*, Istanbul, Turkey, Jun. 11–15, 2006, vol. 9, pp. 4242–4247.
- [15] W. S. Chua, C. Yuen, and F. Chin, "A continuous vector-perturbation for multi-antenna multi-user communication," in *Proc. VTC—Spring*, Dublin, Ireland, Apr. 22–25, 2007, pp. 1806–1810.
- [16] F. Liu, L. Jiang, and C. He, "Low complexity MMSE vector precoding using lattice reduction for MIMO systems," in *Proc. ICC*, Glasgow, U.K., Jun. 24–28, 2007, pp. 2598–2603.
- [17] S. S. Christensen and E. de Carvalho, "Achievable sum-rates in MIMO broadcast channels with vector precoding techniques using coded modulation," in *Proc. VTC—Spring*, Dublin, Ireland, Apr. 22–25, 2007, pp. 2261–2265.
- [18] R. Habendorf and G. Fettweis, "Vector precoding with bounded complexity," in *Proc. SPAWC*, Helsinki, Finland, Jun. 17–20, 2007, pp. 1–5.
- [19] C. Yuen and B. M. Hochwald, "How to gain 1.5 dB in vector precoding," in *Proc. GLOBECOM*, San Francisco, CA, Nov. 27–Dec. 1, 2006, pp. 1–5.
- [20] W. Yao, S. Chen, and L. Hanzo, "Improved MMSE vector precoding based on the MBER criterion," in *Proc. VTC—Spring*, Barcelona, Spain, Apr. 26–29, 2009, pp. 1–5.
- [21] J. Kennedy and R. Eberhart, "Particle swarm optimization," in *Proc. IEEE Int. Conf. Neural Netw.*, Perth, Australia, Nov. 27–Dec. 1, 1995, vol. 4, pp. 1942–1948.
- [22] J. Kennedy and R. C. Eberhart, *Swarm Intelligence*. San Mateo, CA: Morgan Kaufmann, 2001.
- [23] A. Ratnaweera, S. K. Halgamuge, and H. C. Watson, "Self-organizing hierarchical particle swarm optimizer with time-varying acceleration coefficients," *IEEE Trans. Evol. Comput.*, vol. 8, no. 3, pp. 240–255, Jun. 2004.
- [24] L. Hanzo, M. Münster, B. J. Choi, and T. Keller, *OFDM and MC-CDMA for Broadband Multi-User Communications, WLANs and Broadcasting*. Chichester, U.K.: Wiley, 2003.
- [25] S. Chen, A. Livingstone, H.-Q. Du, and L. Hanzo, "Adaptive minimum symbol error rate beamforming assisted detection for quadrature amplitude modulation," *IEEE Trans. Wireless Commun.*, vol. 7, no. 4, pp. 1140–1145, Apr. 2008.
- [26] S. M. Guru, S. K. Halgamuge, and S. Fernando, "Particle swarm optimisers for cluster formation in wireless sensor networks," in *Proc. 2nd Int. Conf. ISSNIP*, Melbourne, Australia, Dec. 5–8, 2005, pp. 319–324.
- [27] H.-M. Feng, "Self-generation RBFNs using evolutionary PSO learning," *Neurocomputing*, vol. 70, no. 1–3, pp. 241–251, Dec. 2006.
- [28] K. K. Soo, Y. M. Siu, W. S. Chan, L. Yang, and R. S. Chen, "Particle-swarm-optimization-based multiuser detector for CDMA communications," *IEEE Trans. Veh. Technol.*, vol. 56, no. 5, pp. 3006–3013, Sep. 2007.

Multisector Eigenbeamforming With MMSE Reception in Spatially Correlated Channels

Jae-Heung Yeom and Yong-Hwan Lee, *Member, IEEE*

Abstract—Single-sector eigenbeamforming is effective for obtaining transmit array gain in spatially correlated fading channels while reducing the feedback signaling overhead. However, it may suffer from interference near the sector boundary when applied to the downlink with universal frequency reuse. This interference may not sufficiently be handled by a minimum mean square error (MMSE)-type receiver. To alleviate the interference problem, we consider the use of multisector eigenbeamforming (MEB) in an MMSE receiver, which requires cooperation between adjacent sectors in the same cell. We analyze the performance of the MEB with the use of long-term channel information in terms of the ergodic capacity. Finally, the effectiveness of the proposed MEB near the sector boundary is verified by computer simulation.

Index Terms—Correlation, eigenbeamforming, interference, minimum mean square error (MMSE) receiver, multisector.

I. INTRODUCTION

The demand for higher throughput has motivated the development of advanced wireless systems that employ multiantenna techniques with universal frequency reuse [1], [2]. Recent measurement results have shown that multiantenna channels are often spatially correlated in real environments [3]. The use of single-sector eigenbeamforming (SEB) is effective in spatially correlated channels while reducing the feedback signaling overhead [4]. However, when SEB is applied to users near the sector boundary, it may experience serious intersector interference problems.

A minimum mean square error (MMSE)-type receiver with short-term channel-state information (CSI) can suppress the interference while reducing the fading effect [5]. A number of studies have been devoted to the design and analysis of MMSE receivers that can maximize the signal-to-interference plus noise ratio (SINR) [5]–[9]. Most of the previous studies considered the MMSE reception with the use of a single transmit antenna under specific conditions (e.g., equal-power interferers) or SEB with perfect CSI. Advanced wireless systems such as mobile Worldwide Interoperability for Microwave Access (WiMAX) and the Third-Generation Partnership Project (3GPP) Long-Term Evolution consider the use of two receive antennas [2], [10]. However, the MMSE receiver cannot properly manage interference sources that are larger than or equal to two [11]. The performance of users near the sector boundary can be improved through sector-cooperative techniques such as softer handover, macrodiversity handover (MD), and fast sector selection (FSS) with muting [12]–[14]. However, these schemes neither consider the use of multiple transmit antennas nor exploit the spatial correlation.

We consider the use of multisector eigenbeamforming (MEB) that requires cooperation between adjacent sectors in the same cell. The proposed MEB can avoid strong interference from adjacent sectors

Manuscript received June 19, 2010; revised September 6, 2010; accepted October 11, 2010. Date of publication November 22, 2010; date of current version February 18, 2011. The review of this paper was coordinated by Dr. T. Taniguchi.

J.-H. Yeom is with the AP Systems Inc., Seoul 153-768, Korea (e-mail: jhyeom@apsystems.co.kr).

Y.-H. Lee is with the School of Electrical Engineering, Seoul National University, Seoul 151-744, Korea, and also with the Institute of New Media and Communications, Seoul National University, Seoul 151-742, Korea (e-mail: ylee@snu.ac.kr).

Digital Object Identifier 10.1109/TVT.2010.2093934